

Vortex Generators Used to Control Laminar Separation Bubbles

M. Kerho,* S. Hutcherson,† R. F. Blackwelder,‡ and R. H. Liebeck§
University of Southern California, Los Angeles, California 90089

This study examines the effect of various forms of vortex generators on the laminar separation bubble of a two-dimensional low Reynolds number Liebeck LA2573A airfoil. The objective of this research was to determine the effects that different generator sizes and spacings have upon the separation bubble and the drag. Wind-tunnel measurements were made on several generator configurations at Reynolds numbers ranging from 200,000 to 600,000 at angles of attack less than the stall angle where the separation bubble can provide a significant contribution to the airfoil drag. The vortex generators used were constructed small enough to be contained completely within the laminar boundary layer. Wind-tunnel data included airfoil drag and mean and fluctuating velocity measurements in the laminar and turbulent boundary layers. Results have shown that the use of vortex generators provides a measurable decrease in airfoil drag at the lower range of Reynolds numbers tested. At the airfoil's design condition and Reynolds number of 235,000, the submerged vortex generators were shown to decrease the airfoil drag by a maximum of 38% at $C_l = 0.572$.

Nomenclature

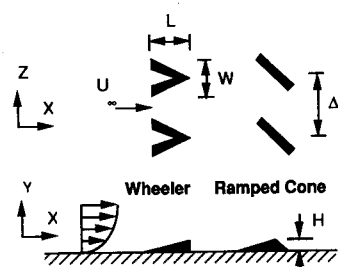
C_d	= airfoil drag coefficient per unit span
C_l	= airfoil lift coefficient per unit span
c	= airfoil chord
H	= maximum height of a vortex generator
L	= streamwise length of a vortex generator
Re_c	= Reynolds number based on the airfoil chord
U_{edge}	= boundary-layer edge velocity
U_∞	= freestream velocity
W	= spanwise width of a vortex generator
x	= chordwise position downstream of the airfoil leading edge
$Y_{30\%}$	= separation bubble height parameter
α	= angle of attack
Δz	= center-to-center spanwise generator spacing
Δz_{cr}	= critical center-to-center generator spanwise spacing
δ^*	= displacement thickness
θ	= momentum thickness

Introduction

SEVERAL current airfoil applications operate in the low Reynolds number regime, including remotely piloted vehicles, high altitude aircraft, compressor blades, and wind turbines. Typically, many of these airfoils operate at a chord Reynolds number of $Re_c < 10^6$ and experience a laminar separation bubble for angles of attack less than the stall angle. The separation bubble is formed slightly downstream of the beginning of the adverse pressure gradient where the laminar boundary layer separates and forms an unstable shear layer which rapidly transitions to a turbulent shear layer. The strong turbulent mixing downstream of the transition promotes the reattachment of the turbulent shear layer. The flow then continues as an attached turbulent boundary layer to the trailing edge.

Although small separation bubbles have been experimentally shown to have little effect upon the airfoil's lift, they can create a thicker turbulent boundary layer resulting in a significant drag increase. A primary goal of this research is to reduce or eliminate the separation bubble through the use of submerged vortex generators, and thus reduce the drag. Although vortex generators have commonly been used to delay separation in turbulent boundary layers, they have rarely (if ever) been used for the same purpose in laminar boundary layers. The vortex generators are located immediately downstream of the airfoil's pressure peak, and are contained completely within the boundary layer. The vortex generators that were tested had heights between 30–80% of the local boundary-layer thickness. They are designed to produce a streamwise vortex that energizes the near wall laminar flow to overcome the adverse gradient. Their shape and small size are intended to prevent the flowfield from becoming turbulent prematurely. The range of interest for this investigation was $200,000 < Re_c < 500,000$ at angles of attack less than the stall angle. This range represents typical operating conditions for a low Reynolds number airfoil.

Several types of generators, sketched in Fig. 1, were used with various spanwise spacings. Wishbone vortex generators designed by Wheeler¹ were tested. These generators consist



Vortex Generator	H	W	L
Dimensions:	(mm)	(mm)	(mm)
Large Wishbone Generators	1.27	6.00	7.70
Small Wishbone Generators	0.48	4.75	4.75
Thin Ramped Cones	0.64	4.80	2.78

Fig. 1 Wheeler wishbone and thin ramped cone generators.

Presented as Paper 90-0051 at the AIAA 28th Aerospace Sciences Meeting, Reno, NV, Jan. 8–11, 1990; received Nov. 17, 1990; revision received March 8, 1992; accepted for publication March 20, 1992. Copyright © 1992 by the American Institute of Aeronautics and Astronautics, Inc. All rights reserved.

*Research Assistant, Aerospace Engineering; currently at The University of Illinois at Urbana-Champaign. Member AIAA.

†Research Assistant, Aerospace Engineering. Member AIAA.

‡Professor Aerospace Engineering. Associate Fellow AIAA.

§Adjunct Professor Aerospace Engineering. Associate Fellow AIAA.

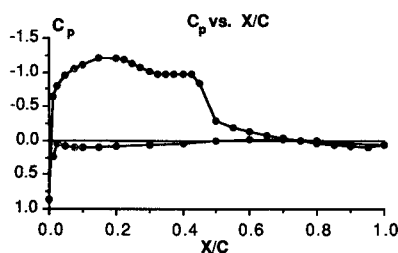


Fig. 2 Airfoil pressure distribution at $Re_c = 235,000$ and $\alpha = 4$ deg, $C_l = 0.572$.

of two joined legs with an included angle of approximately 60 deg with their apex pointing downstream. Two different sizes were tested having apex heights of 1.27 and 0.48 mm. A ramped cone generator designed by the authors was also studied. The ramped cone had its maximum height of 0.64 mm at approximately $\frac{2}{3}$ its length. A conventional transition strip of glass bead grit (0.31 mm) was also tested to provide a comparison with the new generators.

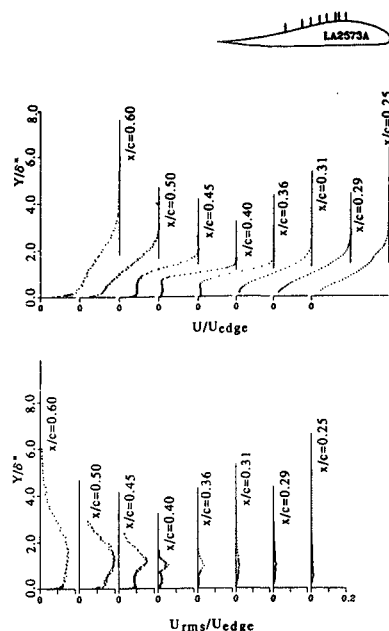
Experimental Technique

The airfoil used for this research, an LA2573A with a 0.298 m chord, was mounted in the 0.94 by 1.27 m semi-hexagonal cross section of the USC Dryden wind tunnel. The tunnel is a closed return type with a contraction ratio of 7:1 and a maximum test section velocity of approximately 34 m/s. A two-dimensional configuration was used with the airfoil spanning the tunnel width. The freestream turbulence level in the test section has been measured to be 0.1%. A pressure distribution of the airfoil is shown in Fig. 2 which shows the separation bubble at approximately $0.30 < x/c < 0.50$.

Streamwise mean and turbulent velocity measurements were taken using a single hot wire probe driven by a constant temperature anemometer. Velocity profile data were taken at an angle of attack of 4 deg and $Re_c = 235,000$ at chord positions ranging from $x/c = 0.15$ to $x/c = 0.99$. Airfoil drag was measured by the momentum defect obtained from a pressure rake in the wake over the range of Reynolds numbers from 200,000 to 600,000 at an angle of attack of 4 deg. From repeatability and comparison to previous results for the clean airfoil, an uncertainty in C_d of approximately 0.001, or 5% can be expected. Drag data were also taken at angles of attack ranging from -2 to 14 deg at a constant Re_c of 235,000. Further experimental conditions are described by LeBlanc et al.² The model used for this experiment was not pressure instrumented. The reported lift coefficients are obtained from a smaller cord airfoil of the same shape and angle of attack which was pressure instrumented. Relatively small separation bubbles at low Reynolds number show that the bubble has a negligible effect upon C_l and $C_{l\alpha}$ thereby justifying this correlation.

Results and Discussion

Before the vortex generators were applied to the airfoil, drag and mean velocity profiles were taken with the clean configuration to document the separation bubble. Boundary layer integral parameters δ^* and θ were calculated directly from the velocity profiles for all cases. Mean velocity profiles and corresponding turbulence intensities for the clean airfoil are shown in Fig. 3. The profiles have been normalized by the displacement thickness to allow easier comparison, and are read from right to left with increasing chord position. The large areas of constant velocity near the wall at positions ranging from approximately $x/c = 0.31$ to $x/c = 0.50$ are indicative of the separation region. Reverse flow regions of the separation bubble are not depicted due to the fact that hot wire anemometer does not indicate flow direction; however, the data does provide a good means for determining bubble location and height. Laminar to turbulent transition of the shear layer above the bubble is clearly indicated by the



x/c	0.25	0.29	0.31	0.36	0.40	0.45	0.50	0.60
δ^*	0.0511	0.0579	0.0888	0.1842	0.3165	0.3285	0.3291	0.3526

Fig. 3 Mean velocity and turbulent intensity profiles for the clean airfoil at $Re_c = 235,000$ and $\alpha = 4$ deg. The profiles are normalized by the displacement thickness.

significant jump in turbulent intensity seen in the bubble region.

The first vortex generators to be applied to the airfoil were the Wheeler wishbone type with a maximum apex height of 1.27 mm, corresponding to approximately 80% of the local boundary-layer thickness. In all cases, the generators were placed directly behind the airfoil's pressure peak as determined from Fig. 2 at a chord position of $x/c = 0.22$. Smaller wishbone generators were also tested having an apex height of only 0.48 mm, or approximately 30% of the local laminar thickness. The third generator tested was a thin ramped cone with an apex of 0.64 mm placed at an angle of 30 deg incidence to the flow. The spanwise spacing, Δz in Fig. 1, was varied for all generator types and sizes to optimize their efficiency. A conventional bead grit transition strip was also placed at $x/c = 0.22$ to provide a direct comparison to the vortex generators.

The 1.27-mm wishbone generators were used at a center-to-center spacing of 14.3 mm, as recommended by Wheeler.¹ The mean velocity and corresponding turbulence intensity profiles for this configuration are shown in Fig. 4 where the profiles are normalized by the new displacement thickness. The mean velocity profiles indicate that there are no obvious or distinct areas of separation. Also, the turbulence intensity profiles indicate that transition does not occur until downstream of $x/c = 0.35$. This data corresponds to a spanwise location which lies behind the apex of one of the vortex generators. Further spanwise examination (which will be presented later) indicated that there were several very small separation bubbles remaining between the generators. Therefore, it could be concluded that the generators reduced the size and magnitude of the separation bubble without inducing premature transition.

Since small separation bubbles were found between each generator, a comprehensive study of the spanwise placement for each set of generators was conducted. Intuition suggests that a reduction of the center-to-center spacing would produce a stronger overall effect and decrease the size of the separation bubble further. However, at a closer spacing of $\Delta z = 7.9$ mm, the generators produced a sufficiently large disturbance which caused premature transition. Although this eliminated

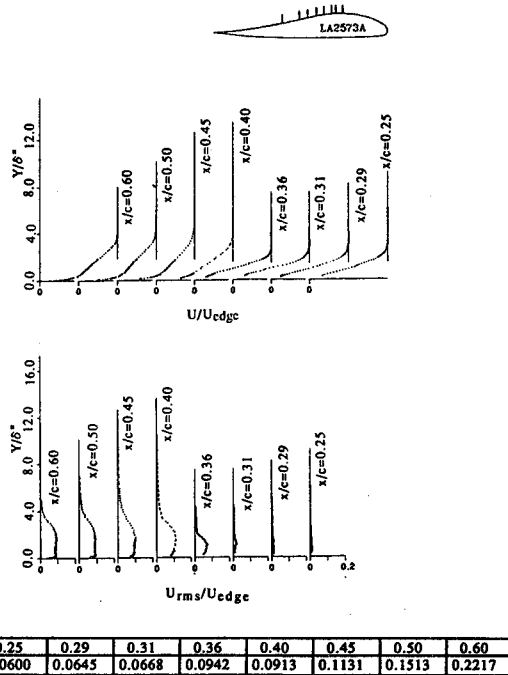


Fig. 4 Mean velocity and turbulent intensity profiles for the airfoil with 1.27-mm wishbone vortex generators at $Re_c = 235,000$ and $\alpha = 4$ deg. The generators are located at $x/c = 0.22$ and have a $\Delta z = 14.3$ mm. The profiles are normalized by the displacement thickness.

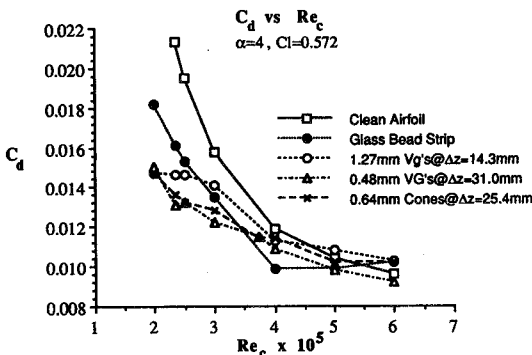


Fig. 5 C_d vs Re_c at 4-deg angle of attack. Comparison of different vortex generator configurations and a glass bead transition strip.

the separation bubble completely, it increased the overall drag and decreased the performance of the airfoil as compared to the original spacing of 14.3 mm. Further examination suggested that a critical spanwise spacing, Δz_{cr} , existed such that for $\Delta z < \Delta z_{cr}$, the generators tripped the boundary layer immediately. Although this eliminated the separation bubble, the resulting turbulent boundary layer increased the total drag. For each set of vortex generators, a range of $\Delta z > \Delta z_{cr}$ was found such that the separation bubble size was reduced and the drag remained near its minimum value. The critical spacing Δz_{cr} differed for each set of generators.

Airfoil drag at the most favorable spacings for each type of generator is shown in Fig. 5 which clearly depicts the favorable results obtained through the use of the submerged vortex generators. A measurable drag reduction was obtained for all three types of vortex generators. At the design conditions of $Re_c = 235,000$ and $\alpha = 4$ deg, the 1.27-mm wishbone generators with $\Delta z = 14.3$ mm produced a 30% drag reduction, the 0.64-mm ramped cones with $\Delta z = 25.4$ mm yielded a 35% drag reduction, and the 0.48-mm wishbone generators with $\Delta z = 31$ mm had a 38% drag reduction. All of the vortex generators eliminated most of the separation bubble; but the smaller physical height of the 0.48 and 0.64-mm generators provided a smaller profile drag and their wider spacing also reduced their device drag more than the larger 1.27-mm generators.

Figure 5 also contains drag data for the glass bead grit transition strip. The conventional transition strip was comprised of 0.31-mm-diam glass beads at the same chord position as the vortex generators. From Fig. 5, the transition strip performs best at a Reynolds number above 375,000. This Reynolds number corresponds to the optimum bead diameter needed to induce transition according to Braslow and Knox.³ Although a 24% drag reduction was seen at the design conditions of $Re_c = 235,000$, increasing the bead size to induce transition at a lower Reynolds number would make the bead's performance unacceptable in the mid and upper range of Reynolds numbers. The vortex generators appear to provide a much larger range of usefulness.

The drag reduction obtained through the use of the vortex generators is also apparent over a range of lift coefficients as shown in the drag polar represented in Fig. 6. A measurable reduction in airfoil drag by the three types of vortex generators is seen over the entire midrange of C_l at $Re_c = 235,000$. This further illustrates the improved efficiency of the vortex generators over the transition strip. The data converges at high C_l near stall because the separation bubble is so small or nonexistent that the generators have very little effect on the airfoil.

A measure of the separation bubble height can be obtained by the distance from the airfoil surface where the velocity is 30% of the local freestream, and will be denoted by $Y_{30\%}$. As used by LeBlanc,⁴ this distance $Y_{30\%}$, is further removed from the airfoil surface than when there is no separation bubble. This parameter allows for a simple comparison of the various generator configurations and types. Velocity profiles at many spanwise and streamwise locations were taken to allow a three-dimensional perspective of the separation bubble. Figure 7 shows a three-dimensional $Y_{30\%}$ isocontour plot for the 0.48-mm wishbone generators with the two-dimensional $Y_{30\%}$ data obtained for the clean model shown for comparison. The vortex generators have greatly reduced the size and magnitude of the separation bubble as evidenced in the figure. The span covered by the plot includes two vortex generators located at $z = 12$ and 42 mm and $x/c = 0.22$. The small separated region located between the generators is clearly evident. The height of the region above the surface is only 0.8 mm compared to the clean case of 3.3 mm. Although the flow due to the vortex generators is more three-dimensional than the two-dimensional clean case, the small regions between the generators are still areas of locally separated flow. A separate visualization study indicated that the small cone, or spike in $Y_{30\%}$, seen at $z = 42$ mm was caused by a strong upward jet created by the converging flow between the legs of the wishbone generators. This cone, however, does not appear over the generator located at $z = 12$ mm. Spanwise testing indicated that the extremely small separated regions created by the generators near their apexes was random and dependent upon minute physical discrepancies between each generator. The $Y_{30\%}$ surface for both generators is relatively the same down-

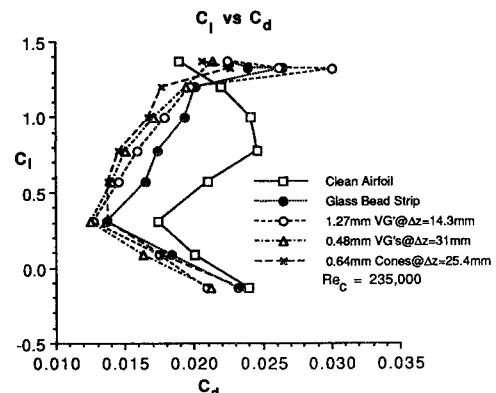


Fig. 6 C_l vs C_d at $Re_c = 235,000$. Comparison of different vortex generator configurations and a glass bead transition strip.

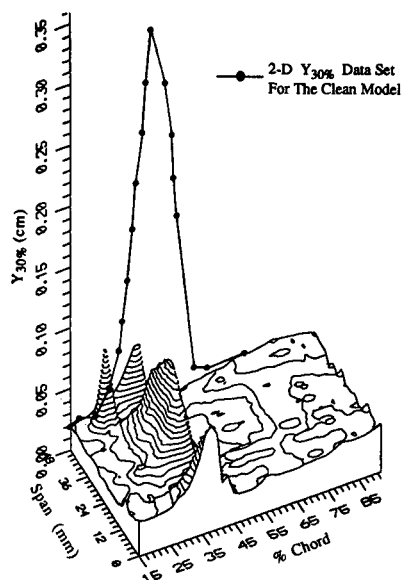


Fig. 7 Three-dimensional isocontour of $Y_{30\%}$ for the 0.48-mm wishbone generators at $Re_c = 235,000$ and $\alpha = 4$ deg.

stream of $x/c = 0.45$. The topographical isocontour map of the data in Fig. 7 is presented in Fig. 8. Again the small locally separated region centered at $z = 26$ mm is apparent between the vortex generators. The figure also shows the separation created over the generator located at $z = 42$ mm. Once more, it is clear that the downstream effect of each generator is similar.

The three-dimensional isocontour plot for the 0.64-mm ramped cones is shown in Fig. 9, again with the two-dimensional clean model data shown for comparison. The random spikes in $Y_{30\%}$ apparent with the 0.48-mm wishbone generators were not seen with the cones because no converging flow is formed. The area covered by the plot includes two generators located at $z = 14$ and 38 mm and $x/c = 0.22$. The simpler design of the wedges provided for better physical consistency in the dimensions of the generators which is apparent in the more uniform effect each generator had on the flow as compared to the 0.48-mm wishbones. The topographical isocontour plot for the wedges is shown in Fig. 10. These generators provide a similar pattern to the wishbones in Fig. 8. Both sets of generators, the 0.48-mm wishbones and 0.64-mm ramped cones, have considerably reduced the size of the clean airfoil separation bubble without adversely affecting the flow or causing premature transition. Since the larger 1.27-mm wishbone vortex generators had a smaller reduction in drag than the 0.48-mm wishbone and 0.64-mm ramped cones, three-dimensional data were not taken for them.

Momentum and displacement thickness were computed and show a marked decrease in the presence of the vortex generators. The momentum thickness θ is a measure of the momentum loss due to the shear force at the surface from the presence of a viscous boundary layer. Since all of the devices produced less drag than the clean airfoil, their momentum thickness was smaller as shown in Fig. 11. This figure suggests that the momentum thickness is relatively constant with little or no separation bubble, i.e., with the vortex generators or transition strip; but it is greatly affected by a large separation bubble as shown by the clean configuration. The momentum thickness for the various vortex generator and transition strip configurations are very similar and begin to differ noticeably only at chord positions greater than $x/c = 0.45$. The turbulence intensity downstream of the bubble in the clean configuration was markedly greater than for any generator or strip configuration. This is associated with the high momentum thickness of the clean configuration after the bubble has disappeared. From Fig. 11, the generator configuration with the lowest overall momentum thickness over the chord range are

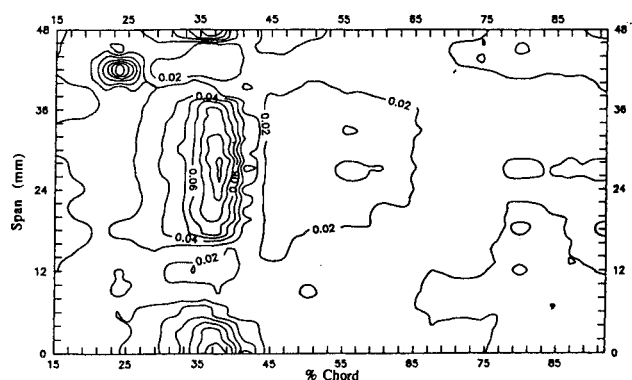


Fig. 8 Topographical isocontour of $Y_{30\%}$ for the 0.48-mm wishbone generators at $Re_c = 235,000$ and $\alpha = 4$ deg. The generators are at 22% chord with $\Delta z = 31$ mm.

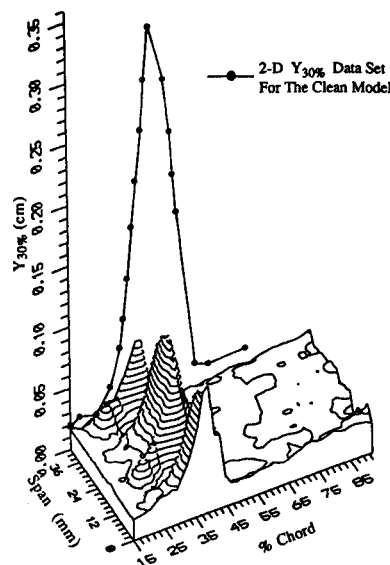


Fig. 9 Three-dimensional isocontour of $Y_{30\%}$ for the 0.64-mm ramped cone generators at $Re_c = 235,000$ and $\alpha = 4$ deg. The generators are at 22% chord with $\Delta z = 25.4$ mm and a 30-deg angle of incidence to the flow.

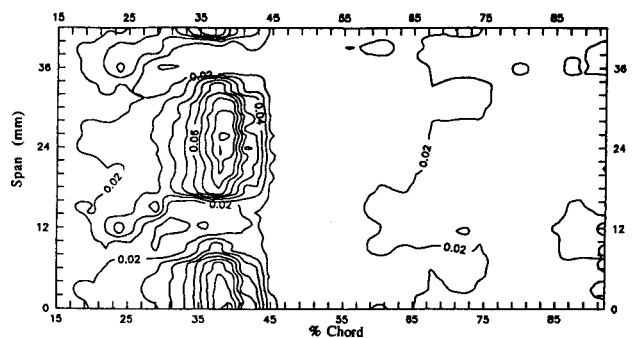


Fig. 10 Topographical isocontour of $Y_{30\%}$ of the 0.64-mm ramped cone generators at $Re_c = 235,000$ and $\alpha = 4$ deg. The generators are at 22% chord with $\Delta z = 25.4$ mm and a 30-deg angle of incidence to the flow.

the 0.48-mm wishbone generators at $\Delta z = 31$ mm. This configuration also provided the largest drag reduction of 38% at the design conditions of $\alpha = 4$ deg and $Re_c = 235,000$.

The displacement thickness δ^* gives the distance that the outer streamlines are displaced by the flow retardation due to the presence of surface shear stress, and is a good representation of the efficiency of the vortex generators. This parameter is plotted for each configuration vs chord position and is depicted in Fig. 12. Before $x/c = 0.30$, where none of the configurations have a substantial separation bubble, the values all correlate well. As the bubble appears in the clean

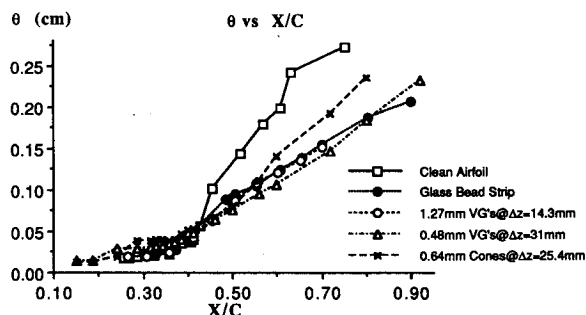


Fig. 11 θ vs X/C at 4-deg angle of attack and $Re_c = 235,000$.

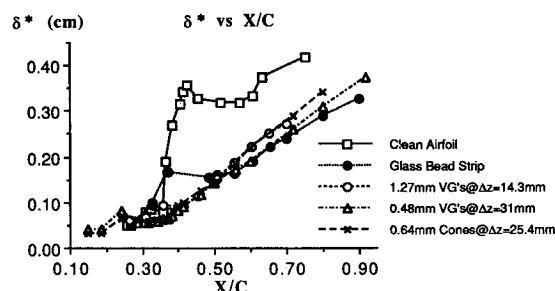


Fig. 12 δ^* vs X/C at 4-deg angle of attack and $Re_c = 235,000$.

configuration, $x/c = 0.31$, the displacement thickness grows rapidly in the presence of the bubble and remains large after reattachment. All of the vortex generator configurations produce a significant reduction in the displacement thickness.

For chord positions ranging from $0.31 < x/c < 0.50$ in the presence of the separation bubble, there is the possibility for error in the calculation of the momentum and displacement thicknesses. Since the hot wire only measures absolute velocity, the reverse flow areas in the bubble are not detected. Therefore, when the boundary layer is integrated the velocities taken in the bubble could be a source of error for the calculation. Uncertainty in the integral parameters δ^* and θ were estimated by examining the degree of scatter in repeated measurements. As shown by LeBlanc⁴ for the test setup used in this experiment, attached laminar flow produced an uncertainty $\Delta\delta^* = 6\%$ and $\Delta\theta = 3\%$. In the regions of separated flow the uncertainty increases to $\Delta\delta^* = 10\%$ and $\Delta\theta = 4\%$. Finally, attached turbulent flow produced uncertainties of $\Delta\delta^* = 2\%$ and $\Delta\theta = 3\%$. The uncertainty in the boundary-layer integral parameters, however, will not effect the conclusions drawn from this research since they are based upon comparative (i.e., not absolute) measurements. Important conclusions drawn from the integral parameters are a result of studying the effect of separation bubble or generator configuration upon the entire upper surface boundary layer. Affects of the separation bubble or generator configuration were shown to largely effect the integral parameters after reattachment where confidence in the measurements was high.

Conclusion

Experimental data from this investigation have shown that the use of submerged vortex generators on the separation bubble of a LA2573A airfoil at low Reynolds numbers sig-

nificantly reduces airfoil drag. This result is confirmed by the 30% drag reduction for the 1.27-mm wishbone generators, the 35% drag reduction for the 0.64-mm ramped cone generators and the 38% drag reduction for the 0.48-mm wishbone generators at the airfoil's design conditions of 4-deg angle of attack and chord Reynolds number of 235,000. At a given chord placement the important design factors appear to include generator height in the boundary layer and center-to-center spacing. This center-to-center spacing Δz is an important parameter and is dependent upon the effect of the stream-wise vortices shed by each generator. Small spacings tend to cause flow disturbances large enough to cause premature transition. Although transition eliminates the separation bubble completely, the resulting premature turbulent boundary layer coupled with the device and profile drag of the generators increases the drag above the case where small separation bubbles are allowed to exist between the generators.

These results are unique because the generators were used in the laminar boundary layer and delayed the onset of the separation bubble. They demonstrated that it is possible to design vortex generators that produce a desirable eddy structure, but yet do it so gently that a turbulent boundary layer is not immediately generated. A smaller separation bubble and a thinner turbulent boundary layer downstream were the result. This result could extend the range and endurance of low Reynolds number aircraft considerably and find use in other applications.

Acknowledgments

This research was supported by the Office of Naval Research under Contract N00014-89-J-1400 monitored by Mike Reischman. The authors would like to thank Patrick LeBlanc for his time, insight, and programming capabilities which greatly enhanced the scope of this project.

References

- ¹Wheeler, G., private communication, Vortex Products, Sumner, WA, 1988.
- ²LeBlanc, P. J., Liebeck, R. H., and Blackwelder, R., "Boundary Layer Performance Characteristics from Wind Tunnel Tests of a Low Reynolds Number Liebeck Airfoil," *Aerodynamics at Low Reynolds Numbers*, Royal Aeronautical Society, London, 1986, pp. 8.1-8.19.
- ³Braslow, A. L., and Knox, E. C., "Simplified Method for Determination of Critical Height of Distributed Roughness Particles for Boundary-Layer Transition at Mach Numbers from 0 to 5," NACA TN 4363, Sept. 1958.
- ⁴LeBlanc, P. J., "An Experimental Investigation of Transitional Instabilities in Laminar Separation Bubble Flows on Airfoils Operating at Low Reynolds Numbers," Ph.D. Dissertation, Dept. of Aerospace Engineering, Univ. of Southern California, Los Angeles, CA, 1992.
- ⁵Liebeck, R. H., "Design and Testing of an Airfoil with Positive Pitching Moment at Low Reynolds Numbers," McDonnell Douglas Rept. MDC18893, 1982.
- ⁶Bell, W. A., and Cornelius, K. C., "An Experimental Investigation of a Laminar Separation Bubble on a Natural Laminar Flow Airfoil," AIAA Paper 87-0485, Jan. 1987.
- ⁷Brendel, M., and Mueller, T. J., "Boundary Layer Measurements on an Airfoil at Low Reynolds Numbers," AIAA Paper 87-0495, Jan. 1987.